中国激光

新型红外非线性光学晶体硒镓钡的性质与应用

孟祥鹤[1,2]，李壮[1,2]，姚吉勇[1*]

[1]中国科学院理化技术研究所，北京 100190；

[2]中国科学院大学，北京 100049

摘要 硒镓钡（$BaGa_4Se_7$）晶体是一种新型宽带隙红外非线性光学材料，其在频率下转换输出中远红外激光方面有着独特的优势和良好的应用前景。国内外研究者对其性质和应用进行了广泛的研究。本文总结了近期关于 $BaGa_4Se_7$（BGSe）晶体的性质表征和激光频率转换方面的研究进展，并展望了未来研究方向。

关键词 激光光学；钡镓硒；性质表征；激光频率转换

中图分类号 O782 **文献标志码** A **doi**：10.3788/CJL202249.0101005

1 引 言

中远红外激光，尤其是能够覆盖 3～5 μm 和 8～14 μm 两个大气窗口的连续可调谐激光，在红外遥感、激光通信、医疗检测和半导体加工等领域都有着广泛的应用[1-4]。红外非线性光学晶体可以通过光参量振荡等频率下转换技术拓展激光波长的范围，将现有的近红外激光（1～2 μm）变频到中远红外波段（3～20 μm），产生可调谐的中远红外激光，在激光技术领域占据着重要地位。

目前商业化的红外非线性光学晶体主要有 $AgGaS_2$（AGS）、$AgGaSe_2$（AGSe）、$ZnGeP_2$（ZGP）等黄铜矿结构材料，它们经过多年的发展，已经可以获得高质量的晶体和器件。然而，一些固有的性能缺陷限制了它们在激光频率转换方面的应用。例如，当泵浦光脉宽为 35 ns、波长为 1.06 μm 时，AGS 和 AGSe 的激光损伤阈值分别只有 25 MW/cm^2 和 11 MW/cm^2，因此不能用于高功率激光泵浦；由于在 1～2 μm 处有较强的吸收，ZGP 不能够使用成熟的 1.064 μm 波段（Nd∶YAG）激光作为泵浦源[5-6]。为了满足中远红外激光的发展需求，亟需综合性能优异的新型红外非线性光学晶体。

$BaGa_4Se_7$（BGSe）是本课题组在 2010 年首次发现并报道的一种新型红外非线性光学晶体[7]。BGSe 属于单斜晶系 Pc 空间群（No. 7），是正双轴晶体，它的结构如图 1 所示：平行排列的 $GaSe_4$ 四面体通过共顶连接，形成三维的网状结构，Ba^{2+} 填充在四面体的网络间隙，与周围的 8 个 Se 原子通过离子键连接，形成双帽三棱柱的配位环境。BGSe 具有较大的带隙宽度（2.64 eV）、宽的透过范围（0.47～18 μm）、大的非线性系数（d_{22} = 24.3 pm/V，d_{23} = 20.4 pm/V，xyz 框架）、适中的双折射率（Δn = 0.06@2 μm）和较高的激光损伤阈值，它可由 1～3 μm的光源泵浦产生长达 18 μm的可调谐

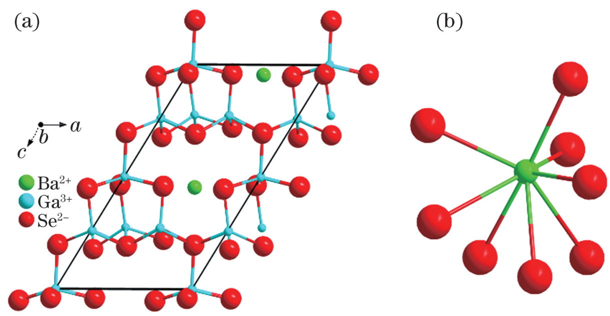

图 1 BGSe 晶体的结构和阳离子配位模式。(a)BGSe 晶体结构；(b)Ba^{2+} 的配位模式

Fig. 1 Crystal structure of BGSe and the coordination mode of cations. (a) Crystal structure of BGSe; (b) coordination mode of Ba^{2+}

收稿日期：2021-08-18；修回日期：2021-09-30；录用日期：2021-10-21

基金项目：国家自然科学基金(51890862)

通信作者：*jyao@mail.ipc.ac.cn

红外激光。与 ZGP 不同，BGSe 不需要经过电子辐照等后处理就可以制备大口径器件，后续的加工工艺比较简单。自此之后，国内外学者围绕 BGSe 的晶体生长及加工工艺、性能表征和激光频率转换进行了大量的研究，取得了许多进展。已经通过光参量放大(OPA)、光参量振荡(OPO)、多种(腔内/腔外，连续/脉冲泵浦)差频(DFG)方式产生高功率、宽波段的红外激光，展示出良好的应用前景。本文总结了近期 BGSe 晶体性质表征和激光频率转换应用方面的研究成果，并对 BGSe 晶体的未来发展进行展望。

2 研究进展

2.1 BGSe 晶体的性质

使用垂直布里奇曼法生长得到的 BGSe 晶体和加工所得器件的典型照片如图 2 所示。透光范围是非线性光学晶体的一个重要参数，它表征晶体的应用波段。对一块厚度为 8.7 mm 的 BGSe 晶体进行透过率测试，结果如图 3 所示。BGSe 晶体在 0.47～18 μm 范围内都具有较高的透过率，能够覆盖 3～5 μm 和 8～12 μm 两个重要的大气窗口；在 15 μm 处有一个由多声子吸收导致的吸收峰。经过计算得到 BGSe 晶体在 4 μm 处的吸收系数为 0.04 cm^{-1}[7]。

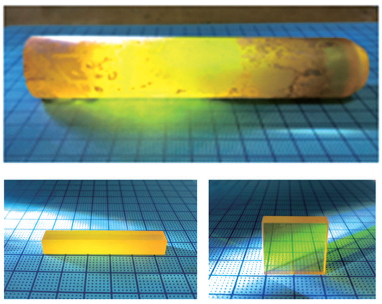

图 2 使用垂直布里奇曼法生长得到的 BGSe 晶体和加工所得器件

Fig. 2 Photographs of BGSe crystal grown by vertical Bridgeman-Stockbarger technique and BGSe devices

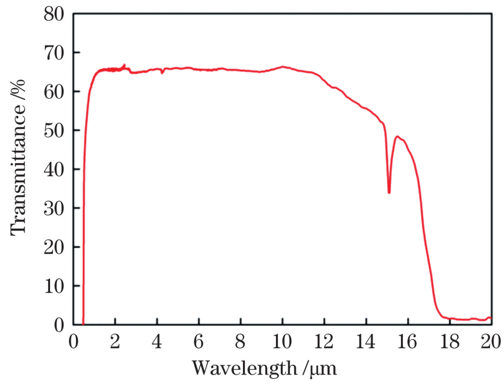

图 3 BGSe 的红外透过率光谱

Fig. 3 IR transmittance spectrum of BGSe

测量折射率的色散曲线，是预测相位匹配特性的先决条件，对非线性光学材料的应用至关重要。国内外多个团队[8-13]使用最小偏转角法和球面法等拟合 BGSe 的折射率色散方程和热光色散方程，拟合结果如表 1 和表 2 所示。

2010 年，Yao 等[7]报道了 BGSe 晶体非线性系数的理论计算值：d_{11} = 18.2 pm/V，d_{15} = −15.2 pm/V，d_{12} = 5.2 pm/V，d_{13} = −20.6 pm/V，d_{24} = 14.3 pm/V，d_{33} = −2.2 pm/V(物理学主轴 XYZ 框架)。2015 年，Zhang 等[14]通过 Maker 条纹法测得了部分非线性系数，但没能得到相对符号。后来，Boursier 等[15]用球面法直接测量了 BGSe 晶体主平面二次谐波和差频产生的相位匹配方向，细化 BGSe 三个主要折射率的 Sellmeier 方程。

表 1 文献[8-10]中拟合的 BGSe 赛米尔方程 $n_i^2=A_{1i}+A_{2i}/(\lambda^2-A_{3i})+A_{4i}/(\lambda^2-A_{5i})$ 和文献[11]中拟合的 BGSe 赛米尔方程 $n_i^2=A_{1i}+A_{2i}/(\lambda^2-A_{3i})-A_{4i}\lambda^2$，其中 $i=x, y, z$，λ 的单位为 μm

Table 1 Fitting Sellmeier equations of $n_i^2=A_{1i}+A_{2i}/(\lambda^2-A_{3i})+A_{4i}/(\lambda^2-A_{5i})$ in Refs. [8-10] and $n_i^2=A_{1i}+A_{2i}/(\lambda^2-A_{3i})-A_{4i}\lambda^2$ in Ref. [11] for BGSe crystals, where $i=x, y$, and z, and λ is in μm

Validity range	n	A_1	A_2	A_3	A_4	A_5	Ref.
0.48–10.4 μm	n_x	7.410040	0.293340	0.051215	1265.119	1896.441	[8]
	n_y	7.323096	0.292889	0.052725	1182.324	1573.474	
	n_z	7.764197	0.326812	0.069734	1297.079	1975.857	
0.5–2.5 μm	n_x	5.952953	0.250172	0.081614	0.001709	–	[11]
	n_y	6.021794	0.256951	0.079191	0.001925	–	
	n_z	6.293976	0.282648	0.094057	0.002579	–	
2–11 μm	n_x	7.405114	0.225316	0.051215	1782.091	1170.528	[9]
	n_y	7.388458	0.224481	0.052725	1778.441	1238.145	
	n_z	7.622884	0.238018	0.069734	1885.307	1303.370	
0.901–10.591 μm	n_x	6.72431	0.26375	0.04248	602.97	749.87	[10]
	n_y	6.86603	0.26816	0.04259	682.97	781.78	
	n_z	7.16709	0.32681	0.06973	731.86	790.16	

表 2 BGSe 的热光色散方程 $dn_i/dT=(B_{1i}\lambda^{-3}-B_{2i}\lambda^{-2}+B_{3i}\lambda^{-1}+B_{4i})\times10^{-4}$(℃$^{-1}$),其中 $i=x, y, z$;λ 的单位为 μm

Table 2 Thermal-optical dispersion equation of $dn_i/dT=(B_{1i}\lambda^{-3}-B_{2i}\lambda^{-2}+B_{3i}\lambda^{-1}+B_{4i})\times10^{-4}$(℃$^{-1}$) for BGSe crystals, where $i= x, y$, and z, and λ is in μm

Validity ranges	dn/dT	B_1	B_2	B_3	B_4	Ref.
25–150 ℃	dn_x/dT	0.6837	1.7607	1.6316	0.0318	[12]
	dn_y/dT	0.2692	0.3112	0.2201	0.4867	
	dn_z/dT	0.7223	1.5170	1.2953	0.1296	
20–120 ℃	dn_x/dT	0.60868	1.26368	1.05624	0.19583	[13]
	dn_y/dT	0.63935	1.31762	1.08950	0.24079	
	dn_z/dT	0.63141	1.30790	1.08486	0.20758	

Kostyukova 等[16]直接在折射率主轴 xyz 框架下定义了有效非线性系数张量分量,并指出 d_{16} 和 d_{23} 具有相同的符号,d_{16} 的数值与 d_{23} 相当,且远大于 d_{15}。Guo 等[17]通过记录相位匹配二次谐波转换效率与基波波长的函数关系,研究了 BGSe 的非线性系数量级和相对符号。不同课题组测得的 BGSe 非线性系数如表 3 所示,其中,在晶体物理框架 XYZ 中得到的结果被转换到 xyz 框架下。然而,通过这些研究预测的 d_{eff} 值均较低,难以解释 BGSe 出色的频率下转换性能[18]。

表 3 BGSe 的非线性系数 d_{ij}(d_{ij} 的单位为 pm/V),所有结果重新调整到 532 nm

Table 3 Nonlinear coefficients d_{ij} of BGSe, with all results rescaled to 532 nm, where d_{ij} is in pm/V

Tensor component	Theory: converted to xyz (assumption)	Maker fringes: converted to xyz	OPO laser experiment, in xyz	Phase-matched SHG, in xyz
$d_{21}=d_{16}$	+5.2	opposite sign to d_{23}, d_{34}	comparable to d_{23}; lager than d_{15}; same sign to d_{23}	5.3 ± 0.8
d_{22}	+18.2	±24.3±1.5	–	6.2 ± 0.9
$d_{23}=d_{34}$	−20.6	±20.4±1.5	–	−14.2±0.8
$d_{31}=d_{15}$	+14.3	–	–	+2.0±0.3
$d_{32}=d_{24}$	−15.2	–	–	−5.0±0.4
d_{33}	−2.2	–	–	–
Ref.	[7]	[14]	[16]	[15,17]

非线性光学材料的激光损伤阈值是指其在单位面积上所能承受的最大激光功率。高的激光损伤阈值是红外非线性光学材料产生高功率激光的重要前提条件。与 AGS、AGSe 相比,BGSe 具有较高的激光损伤阈值,并且有望通过提高晶体质量进一步增大其激光损伤阈值。2012 年,Yao 等[19]测得 BGSe 在脉宽为 5 ns、重复频率为 1 Hz、光斑直径 $D=0.4$ mm 的 Nd:YAG (1.064 μm)激光下的损伤阈值为 557 MW/cm^2,是 AGS (155 MW/cm^2)的 3.6 倍。此后,国内外研究组在不同测试条件下对 BGSe 进行激光损伤阈值测试,结果见表 4。

表 4 BGSe 的激光损伤阈值

Table 4 Laser damage threshold measurements of BGSe

Test condition				Laser damage threshold		Ref.
Wavelength of light source /μm	Pulse width τ /ns	Beam diameter /mm	Repeat frequency f_{rep}/Hz	F_{th}/(J·cm^{-1})	I_{th}/(MW·cm^{-1})	
1.064	5	0.4	1	2.8	557	[19]
2.09	27	–	500	3.3	122.2	[20]
1.064	14	~4	100	1.4	100	[16]
1.053	16	0.2	100	2.04±0.39	254.6	[21]
			150	2.02 ±0.31	252	
			200	1.81±0.25	225.6	
1.053	7.2±0.4	0.15−0.16	100	2.30	319	[22]
	8.3±0.5		500	1.75	211	
	10.0±0.3		1000	1.56	156	

2.2 硒镓钡的应用

近年来，国内外研究者基于 BGSe 晶体完成了包括光参量放大、光参量振荡、差频（腔内/腔外，连续/脉冲泵浦）等多种方式的宽波段红外激光频率转换，其中应用最广泛的是光参量振荡和光参量放大过程，其次是差频过程。目前该晶体的相位匹配方式主要有角度相位匹配和温度相位匹配，其中常用的匹配方式是角度相位匹配，而对温度相位匹配的应用较少。Yang 等[23]于 2013 年首次实现基于 BGSe 晶体的红外激光输出，此后，基于 BGSe 晶体的红外激光频率转换实验不断涌现。近年来的代表性结果（表 5）包括：以 1.064 μm、10 Hz 光源泵浦，通过Ⅰ型角度相位匹配方式实现了 21.5 mJ @3.8 μm 和 1.05 mJ @11 μm 的脉冲激光输出[24-25]；以 2.09 μm、1 kHz 光源泵浦，分别通过Ⅰ型和Ⅱ型角度相位匹配方式产生 5.12 W@4.3 μm 和 0.31 W @ 9 μm 的激光[26-27]；以 2.79 μm、10 Hz 光源泵浦，通过Ⅰ型角度相位匹配方式，产生最大脉冲能量为 3.5 mJ @5.03 μm 的激光[28]；以连续波 1.064 μm 光源和钛宝石激光差频，通过Ⅰ型角度相位匹配方式产生 3.15～7.92 μm 激光[29]。

表 5 近年来 BGSe 晶体激光频率转换实验进展

Table 5 Recent progress in laser frequency conversion experiment of BGSe crystal

Type of experiment	Pump source	Output wavelength	Maximum input-output energy or power	Ref.
OPO	1.064 μm, 10 ns, 10 Hz	8–14 μm	40 mJ@1 μm→1.05 mJ@11 μm	[25]
OPO	1.064 μm, 11 ns, 20 Hz	3.3–4.1 μm	101.3 mJ@1 μm→21.5 mJ@3.8 μm	[24]
OPO	2.09 μm, 16 ns, 1 kHz	8–9 μm	9.58 W@2.09 μm→0.314 W@8.93 μm	[26]
OPO	2.09 μm, 28 ns, 1 kHz	3–5 μm	28 W@2 μm→ 5.1 W@4 μm	[27]
OPO	1.064 μm, 10 ns, 10 Hz	2.7–17 μm	61 mJ@1 μm→3.7 mJ@7.2 μm	[16]
OPO	2.79 μm, 21 ns, 10 Hz	3.94–9.55 μm	18 mJ@2.79 μm→3.5 mJ@5.03 μm	[28]
DFG	850 nm, 50 kHz	3.15–7.92 μm	1.5 W@850 nm→1.41 μW@5 μm	[29]

2020 年以来的最新激光实验结果还包括：

1) Yang 等[27]报道了由重复频率为 1 kHz、输出波长为 2090 nm 的调 Q Ho:YAG 激光器泵浦的Ⅰ型角度-相位匹配光参量振荡器（图 4）。在线形腔条件下，3～5 μm 波段的最大输出功率达到 5.12 W，对应的斜率效率为30.0%，光-光转换效率

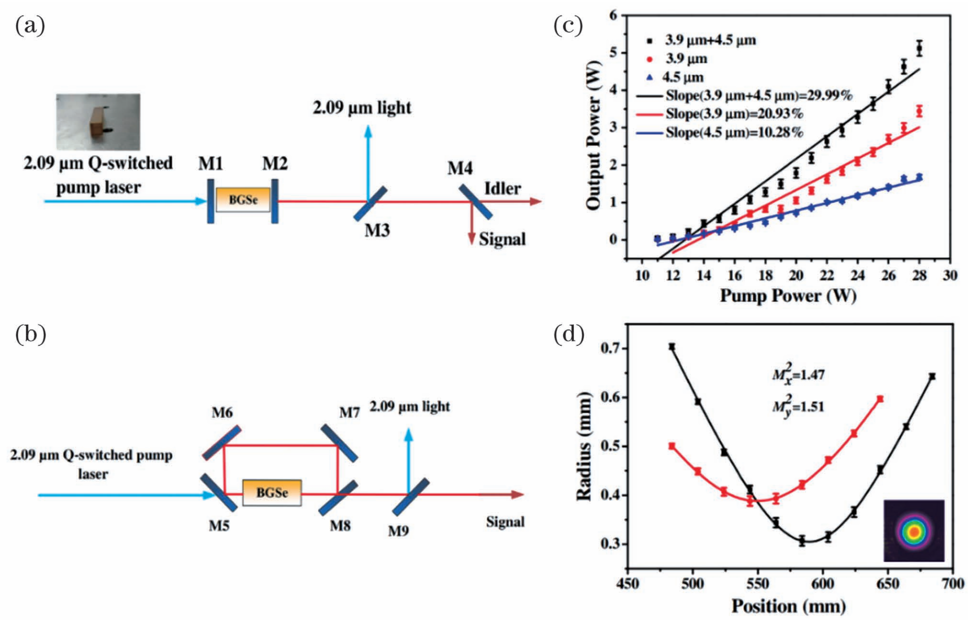

图 4 BGSe 晶体光参量振荡过程原理图[27]。(a)线型腔 BGSe OPO 的示意图；(b)环型腔 BGSe OPO 的示意图；(c)线型腔输出功率与入射泵浦功率的关系；(d)环形腔 OPO 信号光在 x 和 y 方向的光束质量因子 M^2

Fig. 4 Schematic of BGSe-OPO[27]. (a) Schematic of BGSe OPO in a linear cavity; (b) schematic of BGSe OPO in a ring cavity; (c) linear cavity output power versus incident pump power; (d) ring cavity OPO M^2 of signal light in the x and y directions

为 18.3%。在环形腔条件下，获得了输出功率为 3.04 W 的高光束质量红外激光，水平方向和垂直方向的光束质量因子 M^2 分别为 1.47 和 1.51。

2) Zhang 等[30]采用中心波长为 2.4 μm，可输出 28 fs 脉冲宽度的 Cr∶ZnS 激光系统作为泵浦源，使 BGSe 晶体通过Ⅰ型角度相位匹配方式，以脉内差频方式连续产生 6～18 μm 的相干宽带中红外激光，实验装置如图 5 所示。尽管平均功率和转换效率较低，但 BGSe 激光系统输出的光谱带宽明显大于 ZGP(5.8～12.5 μm)和 $LiGaS_2$(6.8～16.4 μm)激光系统输出的光谱带宽。随着聚焦光斑尺寸和晶体厚度的进一步优化，将可以获得更高的平均功率。

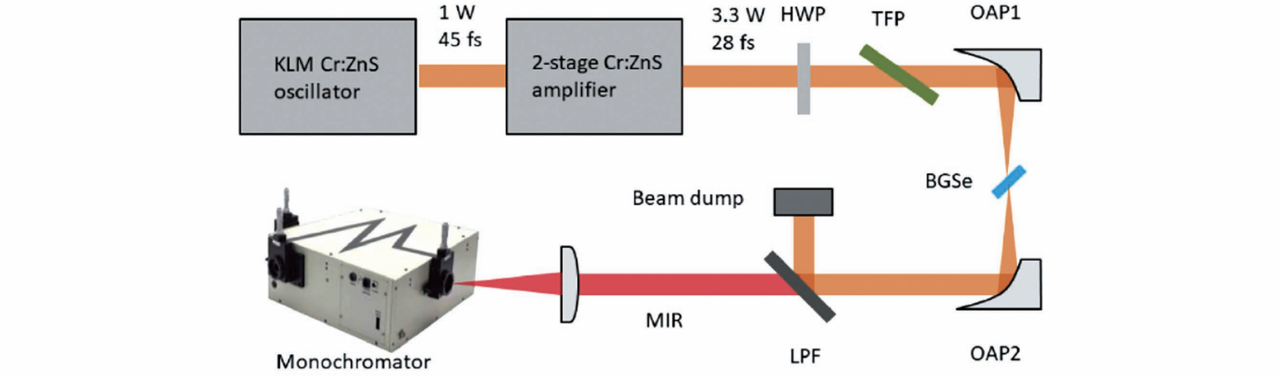

图 5　BGSe 晶体产生中红外激光的实验装置[30]

Fig. 5　Experimental device of MIR generation with BGSe crystal[30]

3)Kong 等[31]提出利用 BGSe 晶体的温度调谐获得红外激光，在满足Ⅰ型相位匹配的条件下，当 BGSe 晶体(56.3°,0°)的温度从 30 ℃升高到 140 ℃时，相应地，闲频光的波长从 3637 nm 增大到 3989 nm，可调谐范围达到 352 nm，$\Delta\lambda_2/\Delta T$ 达到 3.20 nm/℃(图 6)。

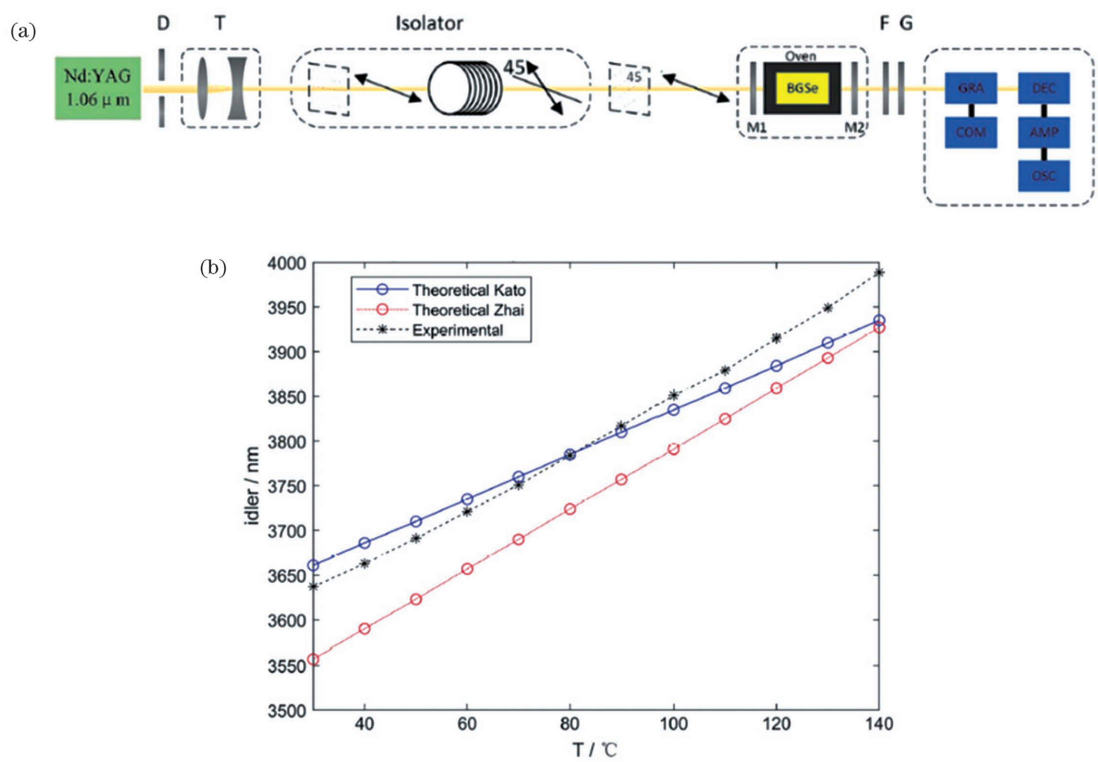

图 6　BGSe 晶体的光参量振荡过程和不同温度下闲频光峰值波长[31]。(a)实验装置示意图；(b) BGSe 晶体(56.3°,0°)在 30～140 ℃范围内的闲频光峰值波长

Fig. 6　OPO process of BGSe crystal and peak wavelength of idle frequency light at different temperatures[31]. (a) Schematic of experimental setup; (b) peak wavelength of idler light of BGSe (56.3°, 0°) at 30–140°C

3 BGSe 晶体和现有红外非线性光学晶体比较

BGSe 晶体和常用红外非线性光学晶体的主要性质对比见表 6，常用的红外非线性光学晶体在激光频率转换中的典型应用见表 7。可以看到：1）在使用 1064 nm 附近光源泵浦产生中远红外激光方面，BGSe 全面超越传统晶体 AGS、AGSe，而 ZGP 和 CdSe 都无法使用 1064 nm 附近光源泵浦。BGSe 是目前最成熟、性能最佳的利用 1064 nm 光源泵浦产生红外激光的晶体，可使用这一波段的光纤激光泵浦。2）在使用 2 μm 附近光源泵浦产生中远红外激光方面，ZGP 在中波大气窗口 3～5 μm 波段的输出功率已达 100 W，但其谱线较宽（150 nm），而且后期需要增加电子辐照工艺，器件口径很难做大（小于 10 mm×10 mm）。ZGP 晶体在长波大气窗口 8～12 μm 波段中 9 μm 以上吸收严重，无法应用。CdSe 晶体可实现 8～12 μm 的激光输出，功率已达 0.8 W@11 μm，但其损伤阈值太低（50 MW/cm²），功率提升空间有限，而且 CdSe 熔点太高且有相变，生长极其困难，晶体的均匀性和重复性较差。BGSe 晶体可通过频率转换产生覆盖 3～5 μm 和 8～12 μm 两个重要大气窗口的激光，目前在两个窗口的输出功率分别达 5 W 和 0.3 W，输出线宽很窄（<10 nm）。BGSe 的优点是晶体损伤阈值高、透光范围宽、输出线宽窄，晶体较易生长，且后期不需要增加电子辐照工艺，可以制作大口径器件（目前已加工出尺寸为 25 mm×25 mm 的器件）；BGSe 的缺点是热导率低，对高重复频率激光的热吸收可能会损坏晶体，针对此问题，可以通过生长高品质的晶体，尽量降低晶体对泵浦光的吸收，从而减弱热效应对晶体的损伤。ZGP 和 CdSe 晶体已经历了 40 多年的发展，在晶体生长和后期加工等方面已接近极致，而针对 BGSe 晶体的研究不到 10 年，在晶体生长、抛光镀膜、激光变频技术等方面还有很大的提升空间，可以进一步提高激光输出功率和能量。

表 6 BGSe 晶体和常用红外非线性光学晶体的主要性质对比

Table 6 Comparison of main properties between BGSe crystal and common infrared nonlinear optical crystals

Crystal	AGS	AGSe	CdSe	ZGP	BGSe
Nonlinear coefficient /(pm·V^{-1})	13	33	18	72	31.5
Laser damage threshold	Low	Low	Low	High	Very high
Pump source /μm*	1–2	1.5–2	2	2	1–3
Output wavelength range /μm*	3–9	3–15	3–18	3–9	3–15
Output line width /nm	10	10	10	150	10
Melting point /℃	993	860	1350	1025	1020
Phase transition	No	No	Yes	No	No
Thermal conductivity /(W·m^{-1}·K^{-1})	1.5	1	6.5	36	0.7
Electron beam irradiation	No	No	No	Yes	No
Ref.	[32]	[33]	[34]	[34]	[7]

Note: *The pump light source and output wavelength range are obtained by comprehensively considering the light transmission range of the material, multi phonon absorption, and refractive index dispersion equation.

表 7 常用的红外非线性光学晶体在激光频率转换中的典型应用

Table 7 Representative laser output results of commonly used infrared nonlinear optical crystals

Crystal	Type of experiment	Pump source /μm	Output wavelength /μm	Maximum output energy or power	Ref.
AGS	OPO	1.064	2.35–5.27	21 mJ@1 μm→0.58 mJ@4 μm	[35]
AGS	DFG	0.780	5–12.5	40 mW@0.780 μm→66 nW@8.06 μm	[36]
AGSe	OPO	1.57	4–8	12 mW@1.57 μm→0.8 mW @4.11 μm	[37]
AGSe	DFG	1.97	6–18	30 mJ@1.06 μm→0.34 mJ@9 μm	[38]
CdSe	OPO	2.097	10.5–12	18.2W@2.097 μm→0.8 W@11 μm	[34]
ZGP	OPA	2.097	3–5	120 W@2.097 μm→102 W@3.92 μm	[39]
ZGP	OPA	2.097	4.3–8.3	116 W@2.097 μm→11.4 W@ 8.3 μm	[40]

Note: $CdGeAs_2$ requires pump light source more than 3 μm, and there have been no reports on laser conversion in recent ten years.

4 结　论

综述了 BGSe 晶体的研究进展，主要包括非线性相关性质的表征结果和红外激光频率转换的研究结果，证明了 BGSe 晶体在非线性光学应用方面具有较大的潜力。与商用化的黄铜矿晶体 AGS、AGSe 相比，BGSe 具有优异的综合性能，包括大的非线性光学系数、宽的红外透过范围、高的激光损伤阈值。与 ZGP 相比，BGSe 适合使用技术成熟的 1 μm 激光进行泵浦，并且能够输出波长为 10 μm 以上的激光，可制出大口径器件。BGSe 晶体在频率下转换输出中远红外激光方面有着独特的优势和良好的应用前景。当然，也有许多亟待解决的问题，主要包括：1）晶体生长方面，仍需改善生长工艺，以获得更高光学质量、更大尺寸的单晶；进一步探索退火方案和条件，降低晶体缺陷，提高红外波段透过率；改善晶体加工、抛光、镀膜工艺，以获得更高激光损伤阈值，减少反射损耗。2）红外激光频率转换性能方面，应解决不同类型泵浦源和 BGSe 晶体光学性质之间的匹配问题，探索最优的相位匹配方向，改良谐振腔结构，以期得到更高质量的红外激光。

参 考 文 献

[1] Liang F, Kang L, Lin Z S, et al. Mid-infrared nonlinear optical materials based on metal chalcogenides: structure-property relationship[J]. Crystal Growth & Design, 2017, 17(4): 2254-2289.

[2] Liang F, Kang L, Lin Z S, et al. Analysis and prediction of mid-IR nonlinear optical metal sulfides with diamond-like structures[J]. Coordination Chemistry Reviews, 2017, 333: 57-70.

[3] Luo X Y, Li Z, Guo Y W, et al. Recent progress on new infrared nonlinear optical materials with application prospect[J]. Journal of Solid State Chemistry, 2019, 270: 674-687.

[4] Petrov V, Badikov V V, Badikov D V, et al. Barium nonlinear optical crystals for the mid-IR: characterization and some applications[J]. Journal of the Optical Society of America B, 2021, 38(8): B46-B58.

[5] Wang W K, Mei D J, Liang F, et al. Inherent laws between tetrahedral arrangement pattern and optical performance in tetrahedron-based mid-infrared nonlinear optical materials[J]. Coordination Chemistry Reviews, 2020, 421: 213444.

[6] Chung I, Kanatzidis M G. Metal chalcogenides: a rich source of nonlinear optical materials[J]. Chemistry of Materials, 2014, 26(1): 849-869.

[7] Yao J, Mei D, Bai L, et al. $BaGa_4Se_7$: a new congruent-melting IR nonlinear optical material[J]. Inorganic Chemistry, 2010, 49(20): 9212-9216.

[8] Badikov V, Badikov D, Shevyrdyaeva G, et al. Phase-matching properties of $BaGa_4S_7$ and $BaGa_4Se_7$: wide-bandgap nonlinear crystals for the mid-infrared[J]. Physica Status Solidi (RRL)-Rapid Research Letters, 2011, 5(1): 31-33.

[9] Boursier E, Segonds P, Ménaert B, et al. Phase-matching directions and refined Sellmeier equations of the monoclinic acentric crystal $BaGa_4Se_7$[J]. Optics Letters, 2016, 41(12): 2731-2734.

[10] Kato K, Miyata K, Petrov V. Phase-matching properties of $BaGa_4Se_7$ for SHG and SFG in the 0.901–10.5910 μm range[J]. Applied Optics, 2017, 56(11): 2978-2981.

[11] Yang F, Yao J Y, Xu H Y, et al. Midinfrared optical parametric amplifier with 6.4–11 μm range based on BaGa4Se_7[J]. IEEE Photonics Technology Letters, 2015, 27(10): 1100-1103.

[12] Zhai N, Li C, Xu B, et al. Temperature-dependent Sellmeier equations of IR nonlinear optical crystal $BaGa_4Se_7$[J]. Crystals, 2017, 7(3): 62.

[13] Kato K, Miyata K, Badikov V V, et al. Thermo-optic dispersion formula for $BaGa_4Se_7$[J]. Applied Optics, 2018, 57(11): 2935-2938.

[14] Zhang X, Yao J Y, Yin W L, et al. Determination of the nonlinear optical coefficients of the $BaGa_4Se_7$ crystal[J]. Optics Express, 2015, 23(1): 552-558.

[15] Boursier E, Segonds P, Debray J, et al. Angle noncritical phase-matched second-harmonic generation in the monoclinic crystal $BaGa_4Se_7$[J]. Optics Letters, 2015, 40(20): 4591-4594.

[16] Kostyukova N Y, Boyko A A, Badikov V, et al. Widely tunable in the mid-IR $BaGa_4Se_7$ optical parametric oscillator pumped at 1064 nm[J]. Optics Letters, 2016, 41(15): 3667-3670.

[17] Guo F, Segonds P, Boursier E, et al. Magnitude and relative sign of the quadratic nonlinear coefficients of the BGSe monoclinic acentric crystal[C]//Laser Congress 2018 (ASSL), November 4-8, 2018, Boston, Massachusetts. Washington, D.C.: OSA, 2018: ATh4A.2.

[18] Zhao X, Li C, Bai J, et al. Recalibration of the nonlinear optical coefficients of $BaGa_4Se_7$ crystal using second-harmonic-generation method[J]. Optics Letters, 2021, 46(23): 5894-5897.

[19] Yao J Y, Yin W L, Feng K, et al. Growth and characterization of $BaGa_4Se_7$ crystal[J]. Journal of Crystal Growth, 2012, 346(1): 1-4.

[20] Yuan J H, Li C, Yao B Q, et al. High power, tunable mid-infrared $BaGa_4Se_7$ optical parametric oscillator pumped by a 2.1 μm Ho∶YAG laser[J]. Optics Express, 2016, 24(6): 6083-6087.

[21] Kolker D B, Kostyukova N Y, Boyko A A, et al. Widely tunable (2.6–10.4 μm) $BaGa_4Se_7$ optical parametric oscillator pumped by a *Q*-switched Nd∶YLiF4 laser[J]. Journal of Physics Communications, 2018, 2(3): 035039.

[22] Kostyukova N Y, Boyko A A, Erushin E Y, et al. Laser-induced damage threshold of $BaGa_4Se_7$ and $BaGa_2GeSe_6$ nonlinear crystals at 1053 μm [J]. Journal of the Optical Society of America B, 2019, 36(8): 2260-2265.

[23] Yang F, Yao J Y, Xu H Y, et al. High efficiency and high peak power picosecond mid-infrared optical parametric amplifier based on $BaGa_4Se_7$ crystal[J]. Optics Letters, 2013, 38(19): 3903-3905.

[24] Zhang Y C, Zuo Y, Li Z, et al. High energy mid-infrared laser pulse output from a $BaGa_4Se_7$ crystal-based optical parametric oscillator [J]. Optics Letters, 2020, 45(16): 4595-4598.

[25] Xu D G, Zhang J X, He Y X, et al. High-energy, tunable, long-wave mid-infrared optical parametric oscillator based on $BaGa_4Se_7$ crystal [J]. Optics Letters, 2020, 45(18): 5287-5290.

[26] Zhao B R, Chen Y, Yao B Q, et al. High-efficiency, tunable 8–9 μm $BaGa_4Se_7$ optical parametric oscillator pumped at 21 μm[J]. Optical Materials Express, 2018, 8(11): 3332-3337.

[27] Yang K, Liu G, Li C, et al. Research on performance improvement technology of a $BaGa_4Se_7$ mid-infrared optical parametric oscillator[J]. Optics Letters, 2020, 45(23): 6418-6421.

[28] Hu S, Wang L, Guo Y, et al. High-conversion-efficiency tunable mid-infrared $BaGa_4Se_7$ optical parametric oscillator pumped by a 2.79-μm laser[J]. Optics Letters, 2019, 44(9): 2201-2203.

[29] Sun M G, Cao Z S, Yao J Y, et al. Continuous-wave difference-frequency generation based on $BaGa_4Se_7$ crystal[J]. Optics Express, 2019, 27(4): 4014-4023.

[30] Zhang J, Wang Q, Hao J, et al. Broadband, few-cycle mid-infrared continuum based on the intra-pulse difference frequency generation with BGSe crystals [J]. Optics Express, 2020, 28(25): 37903-37909.

[31] Kong H, Bian J T, Yao J Y, et al. Temperature tuning of $BaGa_4Se_7$ optical parametric oscillator[J]. Chinese Optics Letters, 2021, 19(2): 021901.

[32] Chemla D S, Kupecek P J, Robertson D S, et al. Silver thiogallate, a new material with potential for infrared devices[J]. Optics Communications, 1971, 3(1): 29-31.

[33] Boyd G, Kasper H, McFee J, et al. Linear and nonlinear optical properties of some ternary selenides [J]. IEEE Journal of Quantum Electronics, 1972, 8(12): 900-908.

[34] Boyd G D, Buehler E, Storz F G. Linear and nonlinear optical properties of $ZnGeP_2$ and CdSe[J]. Applied Physics Letters, 1971, 18(7): 301-304.

[35] Wang T J, Zhang H Z, Wu F G, et al. 3–5 μm $AgGaS_2$ optical parametric oscillator with prism cavity[J]. Laser Physics, 2009, 19(3): 377-380.

[36] Wang L S, Cao Z S, Wang H, et al. A widely tunable (5–12.5 μm) continuous-wave mid-infrared laser spectrometer based on difference frequency generation in $AgGaS_2$ [J]. Optics Communications, 2011, 284(1): 358-362.

[37] Meisenheimer S K, Fürst J U, Buse K, et al. Continuous-wave optical parametric oscillation tunable up to an 8 μm wavelength[J]. Optica, 2017, 4(2): 189-192.

[38] Araki S, Ando K, Miyamoto K, et al. Ultra-widely tunable mid-infrared (6–18 μm) optical vortex source [J]. Applied Optics, 2018, 57(4): 620-624.

[39] Qian C P, Yao B Q, Zhao B R, et al. High repetition rate 102 W middle infrared $ZnGeP_2$ master oscillator power amplifier system with thermal lens compensation[J]. Optics Letters, 2019, 44(3): 715-718.

[40] Qian C, Duan X, Yao B, et al. 11.4 W long-wave infrared source based on $ZnGeP_2$ optical parametric amplifier[J]. Optics Express, 2018, 26(23): 30195-30201.

Property and Application of New Infrared Nonlinear Optical Crystal $BaGa_4Se_7$

Meng Xianghe[1,2], Li Zhuang[1,2], Yao Jiyong[1*]

[1] *Technical Institute of Physics and Chemistry, Chinese Academy of Sciences, Beijing* 100190, *China*;

[2] *University of Chinese Academy of Sciences, Beijing* 100049, *China*

Abstract

Significance Mid-far infrared (IR) laser is widely used in fields such as IR remote sensing, laser communication, medical detection, and semiconductor processing. IR nonlinear optical (NLO) crystal can convert existing near IR lasers (1–2 μm) to mid-far IR range (3–20 μm) through frequency down-conversion technologies, such as optical parametric oscillation (OPO) and optical parametric amplification (OPA). Therefore, exploring mid-far IR NLO crystals that can realize continuous frequency conversion is essential and imminent.

Currently, the commercially available IR NLO crystals are merely restricted to some chalcopyrite-type semiconductors, such as $AgGaS_2$ (AGS), $AgGaSe_2$ (AGSe), and $ZnGeP_2$ (ZGP). It will take years of development to obtain some high-quality crystals and devices. However, some inherent performance defects limit their application in laser frequency conversion. For example, the laser damage thresholds of AGS and AGSe are only 25 MW/cm^2 and 11 MW/cm^2, respectively, under 1.06-μm wavelength and 35-ns pulse width; hence, they cannot be pumped by high-power laser. Moreover, ZGP cannot use the conventional 1.064-μm laser (Nd∶YAG) as the pump source because of its strong absorption in the range of 1–2 μm. New IR NLO crystals with excellent comprehensive properties are urgently needed to meet the development requirements of mid-far IR lasers.

In 2010, we had first discovered and reported $BaGa_4Se_7$ (BGSe) as a new IR NLO crystal. BGSe is a positive biaxial crystal that crystallizes in the monoclinic Pc space group (No. 7), it owns a three-dimensional network structure composed of parallelly aligned $GaSe_4$ tetrahedra with Ba^{2+} in the interstices, and has a large band gap (2.64 eV); wide transmission range (0.47–18 μm); large nonlinear coefficient (d_{22} = 24.3 pm/V, d_{23} = 20.4 pm/V, *xyz* frame); moderate birefringence (Δn = 0.06 at 2 μm); and high laser-damage threshold. It can be pumped by a 1–3-μm light source to produce up to 18 μm of tunable IR laser. Unlike ZGP, BGSe can obtain large-aperture devices without needing to apply electron irradiation treatment. Recently, the BGSe crystal has attracted extensive attention in the terms of crystal growth and processing, property characterization, and laser frequency conversion from researchers at home and abroad. The obtained experimental results explicitly show that the BGSe crystal has good application prospects in high-power and wide-band IR laser frequency conversion via OPO, OPA, and various differential frequency (DFG) methods (e.g., intracavity/out of cavity and continuous/pulse pumping). Hence, summarizing the recent research results of property characterization and laser frequency conversion is very essential and helpful in mastering the future research direction for the BGSe crystal.

Progress In the terms of property characterization, the experimental results obtained by Yao et al. in 2010 showed that the BGSe crystal has a high transmittance that ranges from 0.47 μm to 18 μm, but an absorption peak at 15 μm. Yao et al. also reported the calculated nonlinear coefficients of d_{11} = 18.2 pm/V, d_{15} = −15.2 pm/V, d_{12} = 5.2 pm/V, d_{13} = −20.6 pm/V, d_{24} = 14.3 pm/V, and d_{33} = −2.2 pm/V under the *XYZ* frame. Subsequently, in 2015, Zhang et al. measured partial nonlinear coefficients using the Maker fringe method, but failed to obtain the relative symbol. Thereafter, Boursier, Boulanger, Kostyukova, and Guo. also studied the magnitude and the relative sign of the nonlinear coefficients of BGSe. Table 3 summarizes the nonlinear coefficients of BGSe measured by different research groups. In 2012, Yao et al. measured the damage threshold of BGSe under Nd∶YAG laser (5 ns, 1 Hz, D = 0.4 mm), obtaining a value of 557 MW/cm^2, which is 3.6 times that of AGS (155 MW/cm^2). Since then, the research groups at home and abroad have further studied the laser-damage threshold of BGSe under different test conditions (Table 4).

In the application of laser frequency conversion, Yang et al. realized the IR laser frequency conversion based on the BGSe crystal for the first time in 2013. Thereafter, IR laser frequency conversion experiments based on the BGSe crystal were successively performed. Recently, the representative results include the following: 21.5 mJ at 3.8 μm and 1.05 mJ at 11 μm laser realized by 1.064 μm, 10 Hz pumping source under Type I angle phase

matching; 5.12 W and 0.31 W at 4.3 μm and 9 μm laser realized by 2.09 μm, 500 Hz pumping source under Types I and II angle phase matching, respectively; 3.5 mJ at 5.03 μm realized by 2.79 μm, 10 Hz pumping under Type I angle phase matching; and IR laser in the range of 3.15–7.92 μm produced by differential frequency generation using 1.064 μm and Ti: sapphire laser under Type I angle phase matching. The latest laser experimental results obtained in 2020 include: a coherent broadband mid-IR continuum spanning from 6 μm to 18 μm that was obtained by Zhang et al. using a Cr∶ZnS laser system; and the temperature tuning of BGSe first reported by Kong et al. with a temperature range of 30 ℃ to 140 ℃ and an idler light wavelength of 3637 nm to 3989 nm.

Conclusions and Prospects The BGSe crystal is a new type of wide-bandgap IR NLO material with unique advantages and good application prospects in mid-far IR laser output via the frequency down-conversion process. The future research direction of BGSe mainly focuses on improving the crystal quality, searching for the optimal phase-matching direction, and solving the matching problem between the different types of pump sources and the optical properties of BGSe.

Key words laser optics; BGSe; property characterization; laser frequency conversion